

Emplacement and inflation of natrocarbonatitic lava flows during the March–April 2006 eruption of Oldoinyo Lengai, Tanzania

Hannes B. Mattsson · Jaana Vuorinen

Received: 7 May 2007 / Accepted: 26 May 2008 / Published online: 12 June 2008
© Springer-Verlag 2008

Abstract The most voluminous eruption of natrocarbonatite lava hitherto recorded on Earth occurred at Oldoinyo Lengai in March–April 2006. The lava flows produced in this eruption range from blocky 'a'a type to smooth-surfaced inflated pahoehoe. We measured lava inflation features (i.e. one tumulus and three pressure ridges) that formed in the various pahoehoe flows emplaced in this event. The inflation features within the main crater of Oldoinyo Lengai are relatively small-scale, measuring 1–5 m in width, 2.5–24.4 m in length and with inflation clefts less than 0.4 m deep. Their small sizes are in contrast to a tumulus that formed on the northwestern slope of the volcano (situated ~1140 m below the crater floor). The tumulus is roughly circular, measures 17.5 × 16.0 m, and is cut by a 4.4 m deep axial inflation cleft exposing two separate flow units. We

measured the elastic properties (i.e. shear- and bulk moduli) of natrocarbonatitic crust and find that these are similar to those reported for basaltic crust, and that there is no direct correlation between magmatic head and pressure required to form tumuli. All inflated flows in the 2006 event were confined by lateral barriers (main crater, erosional channel or erosional gully) suggesting that the two most important factors for endogenous growth in natrocarbonatitic lava flows are (1) lateral barriers that prevent widening of the flow, and (2) influx of new material beneath the viscoelastic and brittle crust.

Keywords Natrocarbonatite · Oldoinyo Lengai · Inflation · Pahoehoe · Tumuli · Elastic moduli

Editorial responsibility: A. Harris

H. B. Mattsson (✉)
Institute for Mineralogy and Petrology,
Swiss Federal Institute of Technology (ETH Zürich),
Clausiusstrasse 25, 8092 Zürich, Switzerland
e-mail: hannes.mattsson@erdw.ethz.ch

H. B. Mattsson
Nordic Volcanological Center, Institute of Earth Sciences,
University of Iceland, Askja, Sturlugata 7, 101 Reykjavik, Iceland

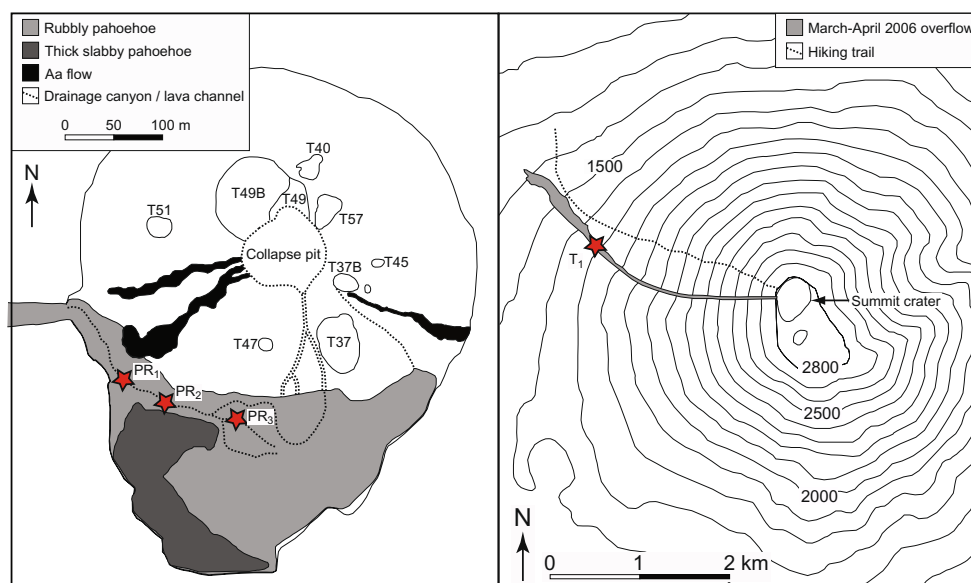
J. Vuorinen
Swedish Museum of Natural History, P.O. Box 50007,
104 05 Stockholm, Sweden

J. Vuorinen
Department of Geology and Geochemistry, Stockholm University,
106 91 Stockholm, Sweden

Introduction

Lava inflation features, such as tumuli and pressure ridges, are common in basaltic lava flow fields on Earth. These types of inflation features occur frequently in both subaerial and submarine settings (Fornari et al. 1978; Walker 1991; Appelgate and Embley 1992; Chitwood 1994; Self et al. 1998; Thordarson and Self 1998; Umino et al. 2000; Duraiswami et al. 2001; Duncan et al. 2004). The process of inflation takes place once a lava flow develops a viscoelastic to brittle crust but is still being supplied with liquid lava from within, resulting in vertical uplift of the flow surface in order to accommodate the inflow of fresh lava (Hon et al. 1994). Tumuli have whaleback-shapes often elongated in the direction of flow, and are frequently cut by both axial and radial inflation clefts (Walker 1991). Pressure ridges are both morphologically and genetically similar to tumuli, but more elongated in the direction of

Fig. 1 Schematic map showing the main lava flows emplaced in the March–April event inside the summit crater (*left*) and on the western flank (*right*). Study locations mentioned in the text is marked with a *star*. Major hornitos are marked as *TXX*, and height curves are in meters. Both maps are modified from Kervyn et al. (2008) which are based on mapping conducted in May 2006



flow. Internal structures characteristic of inflated pahoehoe flows include the three-fold internal morphology (P-type pahoehoe of Wilmoth and Walker 1993) comprising a basal zone rich in short pipe-vesicles, a dense interior and an upper-vesicular crust (Hon et al. 1994; Self et al. 1998; Cashman and Kauahikaua 1997). Hon et al. (1994) showed from measurements of crust thickness in active pahoehoe sheet-flows that there is a positive correlation between crust thickness and the square-root of the time since emplacement. Hon et al. (1994) also suggested that by measuring the crustal thickness in inflated flows, the duration of active uplift can be estimated.

Although inflation features are common in basaltic lava flows, these features have never been described in detail from natrocarbonatitic lava flows. This may in part be because there is only one active natrocarbonatite volcano in the world (i.e. Oldoinyo Lengai), and because Oldoinyo Lengai's sodium-rich lavas react quickly with meteoric water replacing the primary magmatic minerals (gregoryite and nyerereite) with a variety of secondary minerals (Zaitsev and Keller 2006). Thus, most natrocarbonatitic lava flows crumble to dust within a few months of emplacement, and both the surface morphology and internal structures of the lava flows are lost.

Here we describe the morphology of inflation features present in the March–April 2006 lavas of Oldoinyo Lengai. We also show that the elastic moduli of natrocarbonatitic crust are similar to those of basalts. The scarcity of inflation features at Oldoinyo Lengai therefore cannot be attributed to significantly different elastic properties and is more dependent on lateral barriers that prevent widening of the low-viscosity flows in combination with sustained continuous influx of fresh lava.

Chronology of the March–April 2006 eruption

Oldoinyo Lengai is situated in the East African Rift System of northern Tanzania, where it rises approximately 2000 m above the surrounding rift floor. Oldoinyo Lengai has received considerable interest in the literature because it is the only active carbonatite volcano on Earth. For the last 40 years, Oldoinyo Lengai's activity has been characterized by effusion of small-volume natrocarbonatite lavas which have filled and overflowed the summit crater (Fig. 1). In the literature, two main petrographic types of natrocarbonatite lavas have been described (Keller and Krafft 1990; Dawson et al. 1994; Norton and Pinkerton 1997). A crystal-rich, porphyritic, variety of natrocarbonatite has commonly been observed within the main crater. In addition, a phenocryst-poor to aphyric type of lava has also been described, which has been attributed to the process of filter-pressing involving late stage magma derived from the porphyritic lavas (Dawson et al. 1990, 1994).

In March–April 2006 a voluminous overflow of the summit crater occurred, with an estimated bulk volume of $9.2 (\pm 3.0) \times 10^5 \text{ m}^3$ (Kervyn et al. 2008). Although there were conflicting reports on the duration and character of the eruption from media and eyewitnesses, a compilation of these observations in combination with Moderate Resolution Imaging Spectroradiometer (MODIS) satellite data of thermal activity indicate that the lava emplacement spanned March 22nd to April 4th 2006 (Kervyn et al. 2008). A maximum emplacement duration of 14 days yields a mean output rate of $0.76 \text{ m}^3 \text{ s}^{-1}$. However, the peak effusion rates were probably much higher than the mean output rate due to the occurrence of two short-lived episodes of more intense activity (recorded as more intense thermal anoma-

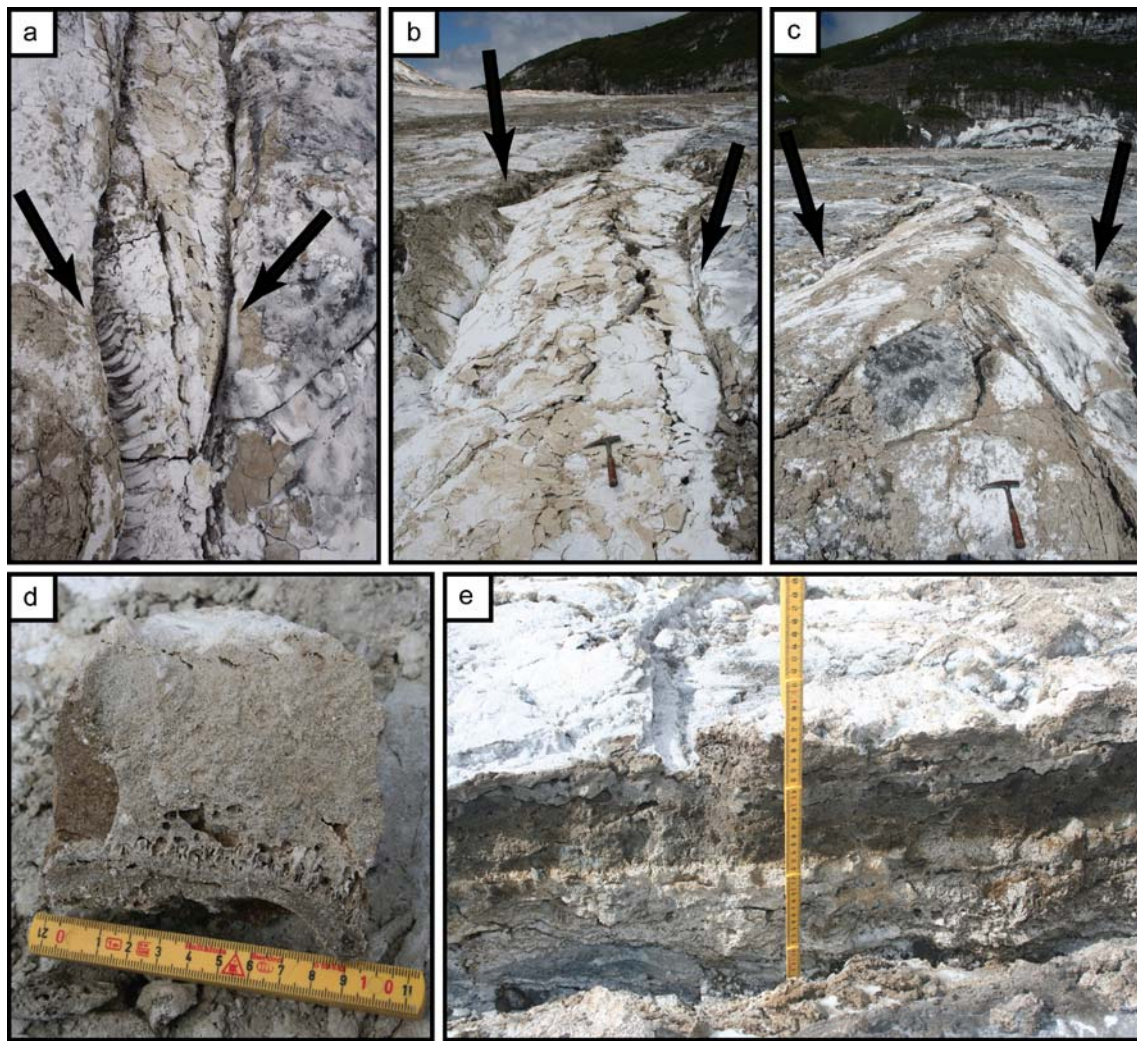


Fig. 2 Photographs showing the general morphology of pressure ridges present inside the main crater of Oldoinyo Lengai. **a** PR₁ from above, **b** PR₂ looking towards SE, **c** PR₃ looking towards SE, **d** cross-sectional view of inflated flow collected between locations PR₁ and

PR₂, **e** inflation cleft with upper vesicular crust at location PR₂. Note that all three pressure ridges are confined inside pre-existing erosional channels (marked by *arrows* in **a–c**)

lies in the MODIS data; Kervyn et al. 2008). Lava filled up the south side of the active crater (where it formed an inflated sheet flow), and subsequently overflowed the western crater rim, extending down a deeply incised erosional gully on the north-western slope of Oldoinyo Lengai (Fig. 1). Before approaching the crater rim, the lava

eroded a channel in the pre-existing, extensively altered, natrocarbonatitic lavas that previously overflowed the rim. The channel is 2.5 m deep, 5 m wide and displays an undercut geometry (Fig. 5f in Kervyn et al. 2008) that has been proposed to be the result of enhanced thermomechanical erosion caused by turbulent flow (Huppert and Sparks

Table 1 Morphological measurements of inflation features in the 2006 eruption of Oldoinyo Lengai

Name	Overall morphology			Axial inflation cleft			Location		
	Length (m)	Width (m)	L/W	Depth (m)	Length (m)	Orientation	Latitude (S)	Longitude (E)	Altitude (m a.s.l.)
PR ₁	2.5	0.47	5.3	0.16	1.17	127°	2°45.634'	35°54.765'	2826
PR ₂	9.6	2.1	4.6	0.36	7.36	086°	2°45.647'	35°54.792'	2827
PR ₃	24.4	4.3	5.7	0.39	16.70	Curved	2°45.649'	35°54.804'	2827
T ₁	17.5	16	1.1	4.43 ^a	10.70	035°	2°45.245'	35°53.601'	1682

^a Combined depth of the two flows (F₁ and F₂) that constitute tumulus T₁. The depth of the inflated flow (F₂) is 2.3 m.

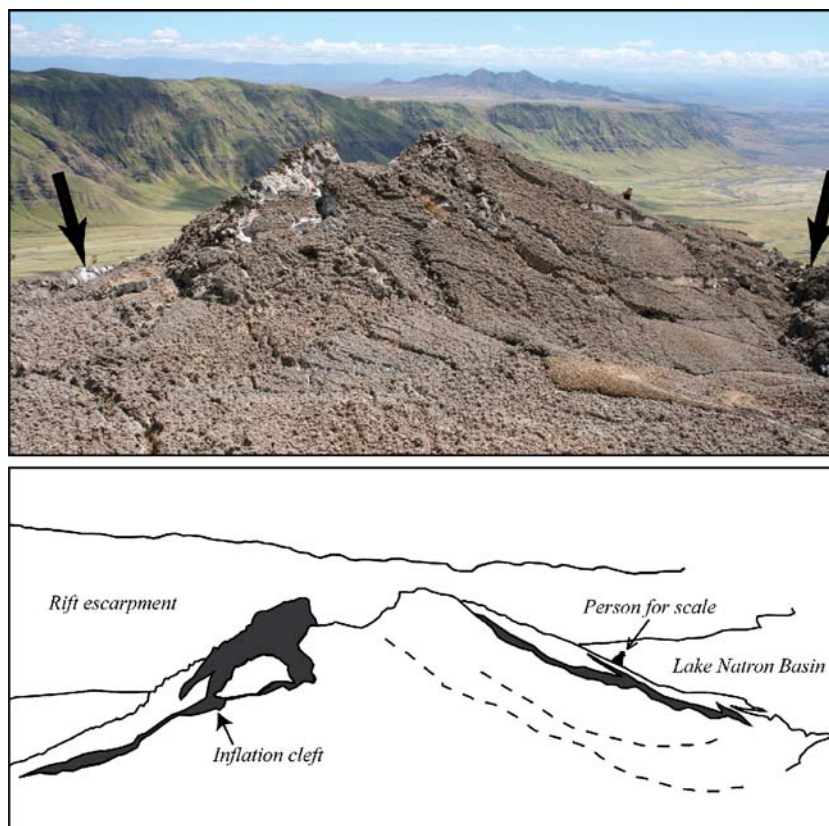


Fig. 3 Photograph and schematic sketch of the large tumulus (T_1) on the NW flank of Oldoinyo Lengai. Note the person for scale and the confinement within an erosional channel (arrows). Dashed lines represent semi-circular slip-surfaces

1985; Jarvis 1995). The overflow finally came to a halt near a settlement at the rift floor, more than 1500 m in altitude below the active crater. A more detailed description of the chronology of events during and after the March–April 2006 eruption of Oldoinyo Lengai can be found in Kervyn et al. (2008).

Results

Morphology of the lava inflation features

We measured three pressure ridges inside the crater and one tumulus on the north-western flank of the volcano (~1140 m below the crater elevation). The three pressure ridges formed within flows emplaced late in the eruption. These flows never reached the crater rim. In contrast, the tumulus formed during a major overflow event associated with higher effusion rates.

Pressure ridges

The three pressure ridges measured in the crater (PR_1 , PR_2 , PR_3 ; Fig. 2a–c) vary in length between 2.5 and 24.4 m, are all relatively narrow with a maximum width of 4.3 m, and have similar aspect (length/width) ratios (Table 1). The

elongated shapes of the pressure ridges are due to lateral confinement within previously formed lava channels (Fig. 2). The depths of the inflation clefts in the pressure ridges range from 0.16 to 0.39 m, with the deepest cleft present in the largest pressure ridge (Table 1). The thicknesses of these lava flows are difficult to estimate because there is no cross-sectional exposure. However, based on the depth of the erosional channel carved by the 2006 lavas into pre-existing altered natrocarbonatites near the crater rim, the thicknesses of these flows does not exceed 2.5 m (c.f. Kervyn et al. 2008).

All three pressure ridges have convex outer surfaces, with the most pronounced curvature present in the thickest flow (i.e., PR_3 ; Fig. 2c). All flows exhibit surface morphologies comprising smooth to ropy pahoehoe lava. Another common feature for all three pressure ridges is the internal morphology comprising a pipe-vesicle bearing base, a dense interior and an upper-vesicular crust (Fig. 2, d and e), similar to basaltic P-type pahoehoe as described by Wilmoth and Walker (1993). Samples collected in the lowermost zone are characterized by pipe vesicles which are often relatively undisturbed, suggesting that the bubbles rose straight upwards and were not affected to any great extent by shear-stress caused by flowing lava. The pipe vesicles are 1–5 mm in width and are commonly 10–45 mm long. The flow interiors are dense with few vesicles and no



Fig. 4 Close-up photographs of various features present in the large tumulus (T_1) in the crater overflow. **a** Inside the axial inflation cleft. The person stands on top of the inflated flow (F_2), another flow (F_1), which does not show any indications of being inflated, caps the

inflated flow. **b** Squeeze-out of lava (white to light gray in color) from the axial inflation cleft. **c** Close up of radial inflation cleft and semi-circular slip-surfaces which form step-like structures. The slip-surfaces are centered on the area in which most uplift occurred

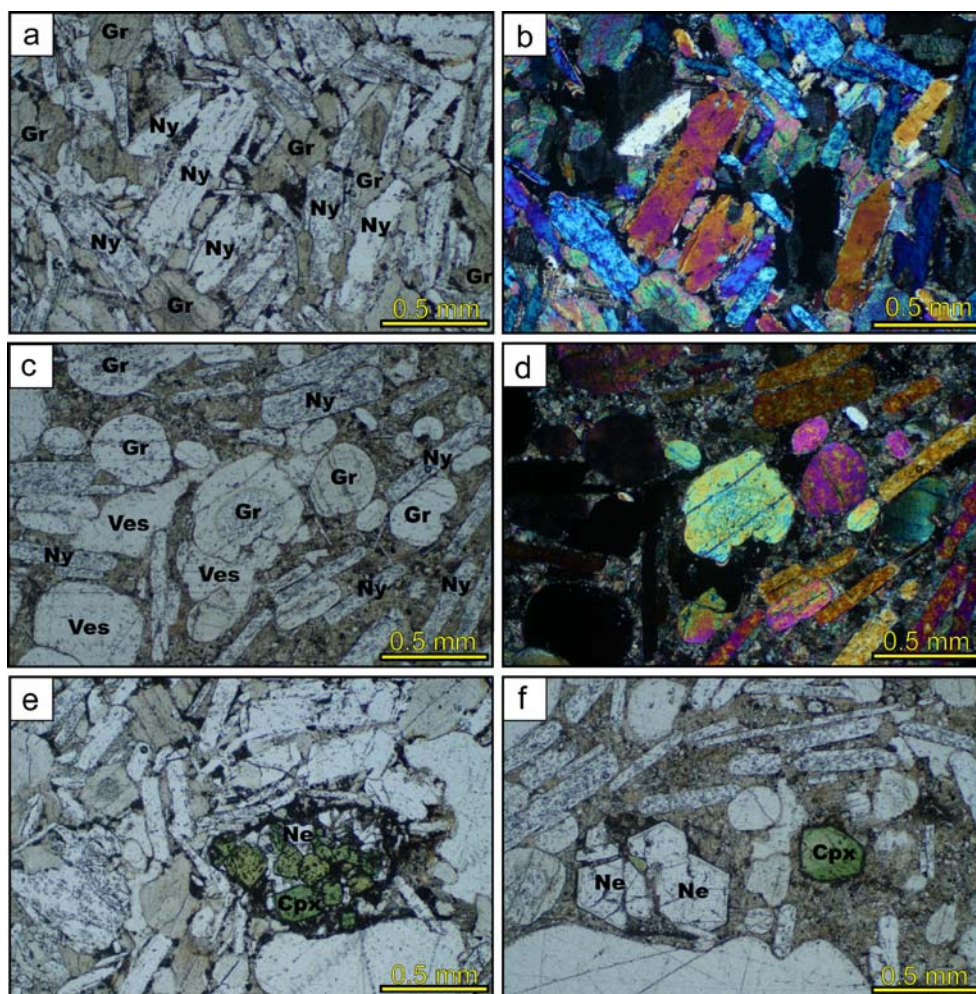
pipe-vesicles or segregation veins. The upper-vesicular crust ranges from a few centimeters in thickness up to >40 cm. In contrast to the pipe-vesicle bearing base, the upper-vesicular crust comprises layers (5–20 mm thick) of deformed vesicles (commonly with a height/width ratio of <0.3). No lava squeeze outs were observed in the inflation clefts, but lava extrusion was recorded as small lobes and toes, displaying “toothpaste” striations (Rowland and Walker 1987), at the flow front.

Tumulus

Although the flank tumulus also formed inside an erosional channel (Fig. 3) it differs markedly in morphology from the

three pressure ridges found inside the crater. The tumulus has a surface texture of rubbly pahoehoe (Guilbaud et al. 2006), and displays a more convex upper surface. The shape of the tumulus is roughly circular with a long axis of ~17.5 m aligned in the flow direction. The 16.0 m width of the tumulus results in an aspect ratio of 1.1 (Table 1). The tumulus is located at a drastic change in slope. The major part of the flow is emplaced on slopes of 30 to 35° (following the steep sides of Oldoinyo Lengai), but the tumulus formed on a 30–40 m long plateau that slopes very gently (<5°). Approximately 100 m further downstream from the tumulus the upper section of a lava tube is exposed (~10° slope). The tube is partially drained and has a radius of at least 1.5 m at this location.

Fig. 5 Thin sections of 2006 overflow lavas. **a** and **b** crystal-rich upper-vesicular crust with lath-shaped nyerereite (*Ny*) grains intergrown with sub-rounded gregoryite (*Gr*) crystals. Note paucity of matrix and vesicles. **c** and **d** textural features of breakout lavas. Matrix is much more abundant as are vesicles when compared to upper-vesicular crust. **e** silicate fragment, composed of clinopyroxene (*Cpx*) and nepheline (*Ne*), in upper-vesicular crust. **f** isolated nepheline and clinopyroxene grains in breakout lavas. Scale bar (0.5 mm) is located at the bottom of each image



An axial inflation cleft (Fig. 4a) and several smaller radial clefts cut the tumulus, from which occasional small breakouts of lava are apparent (Fig. 4b). Inside the axial cleft, two individual flows are exposed (F_1 and F_2 ; Fig. 4a) separated by the rubbly flow-top of F_2 . Inflation clefts cutting several individual flows were also reported by Walker (1991) in some Hawaiian tumuli. The overlying flow (F_1) is 1.8 m thick, whereas the underlying flow (F_2) is at least 2.3 m thick (the total thickness of the flow is not exposed). However, the thickness of the 2006 lavas at this location does not exceed 10 ± 2 m as constrained by the pre-existing topography of the erosional gully (Kervyn et al. 2008). The overlying F_1 -flow was probably emplaced as a breakout from a higher elevation (i.e. higher up in the erosional gully although the absolute source of this flow could not be traced). Flow F_2 represents the main flow emplaced inside the gully. Only the lowermost flow (F_2) has inflated, as the overlying flow (F_1) show no features (on the surface or internally) characteristic of inflation.

An interesting morphological surface feature to note is a set of concentric slip-surfaces (total slip is roughly 10–20 cm) present near the centre of the tumulus where the

maximum uplift occurred (dashed lines in Fig. 3 and close-up in Fig. 4c). The slip surfaces are characterized by striations generated by scraping of brittle crust against a plastic core in response to inflation of the underlying flow (F_2). Plastic behavior of the F_1 -flow is also supported by the convex outer surface of the flow (Figs. 3 and 4c). The inflation cleft in the inflated flow (F_2) is slightly curved and also show striations near the bottom of the cleft, suggesting that the flow was behaving plastically during inflation.

Thin sections prepared of the upper-vesicular crust of the underlying flow display coarse intergrowths of mainly gregoryite and nyerereite (Fig. 5a,b). Nyerereite crystals are aligned subparallel in the direction of flow. Gregoryite crystals are slightly rounded and have inclusion-rich cores and inclusion-free rims. Rounded to subrounded silicate globules occur in various amounts and are composed of euhedral to subhedral nepheline, Ti-andradite and clinopyroxene. They thus correspond to the younger Oldoinyo Lengai stage lava chemistry (Klaudius and Keller 2006). Occasional, isolated silicate grains are also found within the natrocarbonatite matrix. Overall, the petrography is similar to that which has previously been reported for crystal-rich

Table 2 Density and porosity measurements of the March–April 2006 lava

Sample	Length (cm)	Diameter (cm)	Weight (g)	Volume (cm ³)		Density (kg/m ³)		Porosity (%)	
				Bulk	He-pych.	Bulk	He-pych.	Open	Closed ^a
OLT1-T1	3.287	2.514	33.773	16.308	13.196	2071	2559	19.1	0.42
OLT1-T2	2.922	2.523	32.737	14.601	12.838	2242	2550	12.1	0.77
OLT1-T3	3.408	2.538	34.606	17.233	13.580	2008	2548	21.2	0.84
OLT1-S1	3.489	2.555	38.221	17.879	14.985	2138	2551	16.2	0.76
OLT1-S2	3.498	2.540	38.194	17.716	14.976	2156	2550	15.5	0.76

Samples OLT1-TX are cut perpendicular to the vesicle layering, whereas samples OLT1-SX are oriented parallel.

^a Calculated from the measured non-vesicular density of 2570 kg/m³

Lengai lavas (Dawson et al. 1994; Church and Jones 1995). When examined in thin section, the textures of the break-outs differs from the upper-vesicular crust of the tumulus (Fig. 5c, d). Rounded gregoryite and lath-shaped nyerereite crystals have more distinct shapes, the fine-grained ground-mass constitutes 30–40%, and the vesicularity is more variable (from nearly 40 vol. % at the source of the breakout to less than a few percent at the flow front a few meters away). Silicate globules occur, but are less common than in the upper-vesicular crust of the tumulus (Fig. 5e,f). The textural appearance and the mineralogy of the globules are, however, the same.

Measurements of density and porosity of the upper-vesicular crust

The dense rock density of samples from the upper-vesicular crust of the tumulus was obtained by crushing and grinding three small blocks into a fine grained-powder in an agate mortar (thus eliminating all isolated/closed vesicles in the samples). With a known weight, the volumes of the three powder-samples were measured using a helium pycnometer. These measurements yielded an average density of 2570 (± 7) kg m⁻³ based on four measurements.

Bulk densities and open porosities were then measured for five cylindrical samples and their closed porosities were calculated by accounting for the dense rock density measured for the ground rock powders (Table 2). The bulk densities of the samples range from 2008 to 2242 kg m⁻³ (average 2123 kg m⁻³; Table 2). The bulk densities of our samples largely overlap with the 1150–2200 kg m⁻³ range of Pinkerton et al. (1995). The slightly higher densities of our samples can be explained by the fact that the 2006 overflow contains globules of denser combeite- and wollastonite-bearing nephelinites. This makes the overall density higher than for normal natrocarbonatites. For all measured samples the closed porosity is less than 1% (Table 2), indicating that the vesicles are almost completely interconnected in bands forming in the upper-vesicular crust.

Elastic properties of natrocarbonatitic crust

In order to understand the mechanics behind formation of the inflation features it is of importance to know the elastic properties of natrocarbonatitic crust. Because there is no previous experimental determination of these properties we measured them for the first time using an internally heated gas apparatus (Paterson Rig) at ETH Zürich with the experimental assemblage described in Burlini et al. (2005) and Ferri et al. (2007).

Experimental setup

A large sample from the upper-vesicular crust of the T₁-tumulus was prepared by dry-cutting it into several smaller cubes (~50 mm sides), these were mounted on a lathe to produce cylindrical rods with a diameter of 25.4 mm. Three rods were prepared perpendicular to the vesicle layering and three samples parallel to the layering. The rods were dry polished at the end-surfaces for attaining ± 10 μ m ruggedness. One sample oriented with the long axis parallel to the layering (OLT1-S2) and one sample oriented perpendicular to the layering (OLT1-T2) were chosen for analysis. This was done in order to account for different travel times in the most important directions as a certain degree of anisotropic behaviour is to be expected from the vesicle-layering in the samples. We performed a series of experiments in which we measured the travel time of P- and S-waves (i.e. V_p and V_s) through the two samples (derived from 1 MHz forced vibrations) in a pressure range between 10 and 150 MPa (with 10 MPa increments) and at ambient temperature (297 K). The travel times were measured both for increasing and decreasing pressure.

Results

The seismic measurements display some minor scatter but have similar trends for both samples (Fig. 6). This is clear from the relatively stable ratios of V_p/V_s for the two

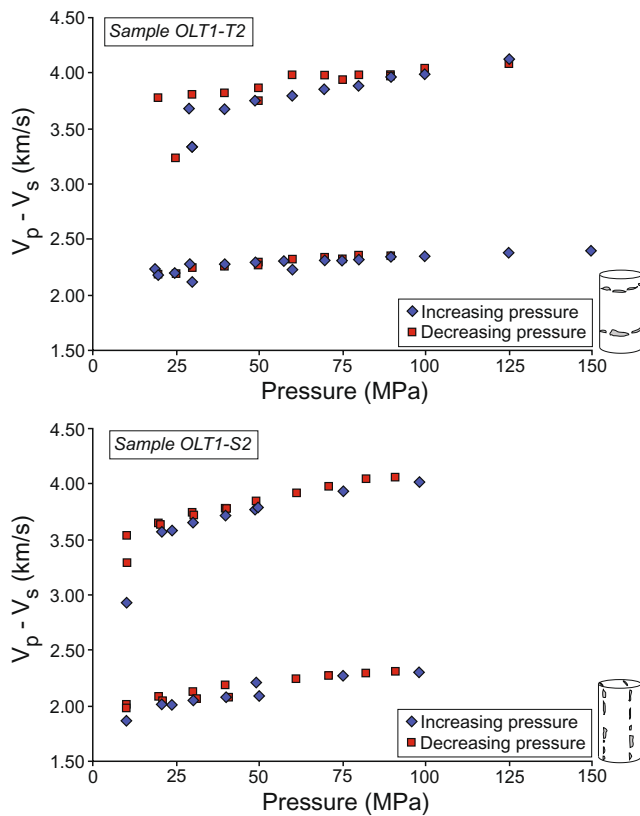


Fig. 6 Seismic wave velocities (P and S wave velocities, V_p and V_s respectively) through samples of the upper-vesicular crust of the tumulus at location T_1 determined from multiple experimental runs in an internally heated gas apparatus (Paterson rig) at ETH Zürich with variable pressure (10 to 150 MPa), with forced vibrations of 1 MHz and a fixed temperature of 25°C. The upper velocities in both diagrams correspond to the P-waves and the lower velocities to the S-waves. Note that sample OLT1-T2 is cut perpendicular to the vesicle layering and sample OLT1-S2 is cut parallel to the same layering in order to account for anisotropic behavior due to the presence of sub-horizontal vesicle bands in the upper-vesicular crust

samples (Table 3). Generally the measurements made with decreasing pressure are more stable than compared to increasing pressure runs. This is a result of closure of microcracks and microporosity in the samples at higher

pressures and, therefore, only the decreasing pressure data were used to determine dynamic modulus for the upper-vesicular crust. The bulk modulus is determined by least-squares regression fitting to the linear portion of the data (e.g. pressures above 30 MPa; Fig. 6). Once the corrected travel times of P- and S-waves are known several elastic parameters can be calculated for the natrocarbonatitic crust (following Birch 1961).

At 25 MPa the corrected P- and S-wave velocities are 3.73 and 2.19 km s⁻¹ respectively. Including these values in the conversions of Birch (1961) yields, for fresh natrocarbonatitic crust, bulk and Young’s moduli of 16.50 and 26.14 GPa, respectively. The Shear modulus is 10.54 GPa and the Poisson’s ratio is 0.24. The natrocarbonatite crust thus displays similar Young’s modulus (i.e. stiffness) as Holocene basaltic lava flows from Iceland (8–33 GPa; Oddsson 1984; Gudmundsson and Philipp 2006), with almost identical Poisson’s ratio (which for basalts range between 0.2 and 0.3; Gudmundsson 2004; Gudmundsson and Philipp 2006).

Discussion

Elastic properties of natrocarbonatitic crust and formation of inflation features at Oldoinyo Lengai

Rossi and Gudmundsson (1996) proposed a mechanical model for tumulus growth based on vertical deflection of a circular elastic plate, which has a supported edge and is subject to uniform magmatic overpressure at the base. In the model of Rossi and Gudmundsson (1996), the magmatic overpressure (P_m) required to form the uplift is defined as:

$$P_m = \frac{64D\omega_{max}}{a^4} \frac{1 + \nu}{5 + \nu} \tag{1}$$

ω_{max} is the maximum deflection of the crust (m) occurring at $r=0$, the radius of the tumulus is denoted by a , ν is the

Table 3 Corrected average wave velocities (km/s) for natrocarbonatitic crust (at 297 K)

Sample #	Wave	Pressure (MPa)											
		10	20	30	40	50	60	70	80	90	100	125	150
OLT1-T2	P	–	3.77	3.79	3.81	3.80	3.97	3.98	3.97	3.98	4.03	4.08	4.16
OLT1-T2	S	–	2.18	2.24	2.27	2.28	2.31	2.32	2.34	2.35	2.35	2.37	2.39
OLT1-S2	P	3.44	3.65	3.73	3.78	3.87	3.95	3.98	4.05	4.06	–	–	–
OLT1-S2	S	2.01	2.07	2.11	2.15	2.23	2.27	2.28	2.30	2.31	–	–	–
OLT1-T2	P/S	–	1.73	1.69	1.68	1.67	1.72	1.71	1.70	1.70	1.72	1.72	1.74
OLT1-S2	P/S	1.71	1.76	1.77	1.76	1.73	1.74	1.75	1.76	1.76	–	–	–

Sample OLT1-T2 are cut perpendicular to the vesicle layering, whereas sample OLT1-S2 is oriented parallel.

Poisson's ratio of the crust, and D is the flexural rigidity of the crust (N m), defined as:

$$D = \frac{Eh^3}{12(1-\nu^2)} \quad (2)$$

Where E denotes the Young's modulus of the lava crust (Pa), and h is the thickness of the viscoelastic crust (m). Rossi and Gudmundsson (1996) also suggested that the magmatic overpressure (P_m) in a tumulus is related to the magmastatic head (P), assuming closed tubes and no leakage, where P equals:

$$P = \Delta z g \rho_m \quad (3)$$

Here Δz is the elevation difference between the entrance to the lava tube and the measured inflation feature, g is the acceleration due to gravity, and ρ_m is the density of the magma.

Using the average value for density (2123 kg m⁻³; Table 2) and $g=9.81$ m s⁻², a maximum magmatic pressure (i.e., P) can be calculated for tumulus T₁ using Eq. 3. The elevation difference between the point source of the tube (located near the crater rim) and Tumulus T₁ is approximately 1140 m. Theoretically, the maximum magmatic pressure that can be generated within a tube beneath the tumulus is thus 23.7 MPa (provided that the tube is closed and no leakage occurs). Rossi and Gudmundsson (1996) concluded that the pressure range required to form tumuli in basaltic lava flows on Icelandic shield volcanoes is in the order of 0.2–1.0 MPa, with a maximum of 2.5 MPa. Similar results were also reached by measurements of tumuli and pressure ridges in the Helgafell lava field in Iceland (average 0.53 MPa; Mattsson and Höskuldsson 2005). However, both the study by Rossi and Gudmundsson (1996) and that by Mattsson and Höskuldsson (2005) used a very low value for the Young's modulus (i.e., 5 GPa). The calculated magmatic overpressure of 23.7 MPa that can be generated in a closed lava tube at the location of the T₁-tumulus is an order of magnitude higher than calculated for tubes on basaltic shield volcanoes in Iceland (Rossi and Gudmundsson 1996), which is mainly a result of the large elevation difference at the steep-sided Oldoinyo Lengai cone compared to the more gently sloping Icelandic volcanoes.

Similar to most physical models, the mechanical model of Rossi and Gudmundsson (1996) has some simplifications. As pointed out by Duncan et al. (2004) the model assumes a circular uplift of the tumuli, which do not fit to the vast majority of tumuli, as they are considerably more elongated in the direction of flow (Walker 1991; Rossi and Gudmundsson 1996; Duncan et al. 2004). However, as the flow-lobe tumulus (T₁) measured on the NW slope of Oldoinyo Lengai is semi-circular in shape (i.e. a length/width ratio of 1.1; Table 1) and in the absence of a better model, a circular approximation is considered acceptable

and we therefore compare our data from Oldoinyo Lengai with the model of Rossi and Gudmundsson (1996).

Solving Eq. 1 with the values measured on tumulus T₁, the experimentally determined flexural rigidity and assuming a similar thickness of the viscoelastic crust as in basaltic lavas (i.e. 0.2 to 0.4 m; Rossi and Gudmundsson 1996), we find that the pressure required to form the T₁-tumulus ranges between 0.27 and 2.19 MPa ($E=26.14$ GPa, $h=0.2-0.4$ m, $\omega_{\max}=4$ m, $\nu=0.24$, and $a=8$ m). The results show that the calculated magmastatic pressure resulting from transport in a tube down the slopes is between one to two orders of magnitude higher than the pressure needed to deflect the crust and form the T₁-tumulus. We conclude that the magmastatic head inside the lava tubes does not directly relate to the formation of inflation features at Oldoinyo Lengai as a magmatic overpressure (0.27–2.19 MPa) inside the lava tube could also be generated by an increased volumetric influx of lava (corresponding to an increase in the volumetric effusion rate).

Duncan et al. (2004) also noted that some tumuli formed in the 1983 eruption of Etna could be explained by the Rossi and Gudmundsson (1996) model while other tumuli could not. There are some general simplifications in the model that might explain why there are problems to fit the model to the actual field observations. We find that the most questionable assumption in the model is that the pressure causing uplift is uniform during the inflation process. In order to maintain a uniform pressure inside a tube or flow lobe it follows that the lava supply rate must also be constant. This is not the case in most, if not all, effusive volcanic eruptions. The 2006 eruption of Lengai, with effusion rate varying more than one order of magnitude, would definitely not be subject to a uniform pressure at the base of any of the recorded inflation features. However, despite the somewhat failing correlation of pressure-results (P_m and P) yielded by Eqs. Eq. 1 and 3 we still consider the tumuli-growth model of Rossi and Gudmundsson (1996) to be valid. This is because we do not now know when/or the tube system was broken (a break in the tube system is suggested by the F₁-flow (Fig. 4a), which overlies the inflated F₂-flow).

In the March–April 2006 eruption, inflation features *only* formed where there were lateral barriers preventing widening of the flows (e.g., inside the main crater, in pre-existing thermally eroded channels or in the erosional gully on the flank). Rossi and Gudmundsson (1996) also noted that *topographic confinement seems essential in the formation of flow-lobe tumulus* in Iceland. The lateral barriers seem to be even more important in natrocarbonatitic lava flows due to the exceptionally low viscosities of the natrocarbonatitic lavas which, if emplaced on a flat to gently sloping surface without barriers, will widen rather than inflate. In addition to this, most eruptions of Oldoinyo Lengai involve small

volumes of lava and continuous effusion is not sustained over a significant period of time which is required for inflation to occur.

Conclusions

The March–April 2006 eruption of Oldoinyo Lengai was hitherto the largest effusive eruptive episode of natrocarbonatite magma ever recorded in the volcano's history. With the largest volume of natrocarbonatitic magma erupted during a single event and also the highest volumetric effusion rate, the resulting lava flows differ in morphology and mode of emplacement from those commonly formed in small-volume breakouts generated by hornito collapse or hornito spill-over.

Lava flows confined within the crater forms an inflated sheet-flow, covering roughly one third of the crater, in which small channels were carved out by thermomechanical erosion. When the flows emplaced during the major overflow events approached, and overflowed, the crater rim they eroded a 2.5 m deep and 5 m wide channel in the pre-existing natrocarbonatites and continued flowing down the north-western slope of the volcano. The overflow was channelized within a pre-existing gully down the steep flank of Oldoinyo Lengai and started to inflate once it reached more gentle slopes near the base of the volcano. Three pressure ridges formed within the summit crater in a late stage of the eruption and these flows never reached the crater rim.

We find no direct correlation between the magmastatic pressure that might be generated inside a closed tube and the pressure required to form the observed uplift (e.g., the values differ up to two orders of magnitude). Hence, we conclude that the most important factor controlling tumulus and pressure-ridge formation is not the magmastatic head but rather the presence of lateral barriers which prevent lateral expansion of any flow (e.g. widening), and instead promotes endogenous growth and inflation. In addition to this, the natrocarbonatitic lava flows need to be supplied with sustained influx of fresh magma over a sufficiently long period of time.

Many previous lava flows at Oldoinyo Lengai were also probably inflated. The difficulty is, however, to record the resulting structures as natrocarbonatite lavas rapidly react with meteoric water and the primary magmatic minerals are rapidly replaced by secondary minerals. Thus, the majority of the flows that are emplaced are transformed into dust within a few months of emplacement and their history lost from the geological record.

Acknowledgements The fieldwork to conduct the present study was funded by research/travel grants from the Swedish Research Council (VR), Nordic Volcanological Center (NORDVULK), and the Royal

Swedish Academy of Sciences (KVA). Fabio Ferri and Luigi Burlini assisted with the analyses of mechanical properties of natrocarbonatitic lavas at ETH Zürich. Matthieu Kervyn, Jurgis Klaudius, Luca Caricchi, Alex Teague and Peter Ulmer are gratefully acknowledged for many interesting discussions on various aspects of Lengai volcanism. HBM would also like to thank Melanie Finn and Matthew Aeberhard for their generous hospitality during the 2007 visit to the Lake Natron area. Finally, we would also like to thank Andreas Jallas (for excellent dry-preparation of thin sections). Insightful reviews by Laszlo Keszthelyi and an anonymous reviewer are gratefully appreciated.

References

- Appelgate B, Embley RW (1992) Submarine tumuli and inflated tube-fed lava flows on Axial Volcano, Juan de Fuca Ridge. *Bull Volcanol* 54:447–458
- Birch F (1961) The velocity of compressional waves in rocks to 10 kbar, Part 2. *J Geophys Res* 66:2199–2224
- Burlini L, Arbaret L, Zeilinger G, Burg J-P (2005) High-temperature and pressure seismic properties of a lower crustal prograde shear zone from the Kohistan Arc, Pakistan. In: Bruhn D, Burlini L (eds) *High-Strain Zones: Structure and Physical Properties*. *Geol Soc Lond Spec Publ* 245:187–202
- Cashman KV, Kauahikaua JP (1997) Reevaluation of vesicle distributions in basaltic lava flows. *Geology* 25:419–422
- Chitwood LA (1994) Inflated basaltic lava: examples of processes and landforms from central and Southeast Oregon. *Oregon Geol* 56:11–20
- Church AA, Jones AJ (1995) Silicate-carbonate immiscibility at Oldoinyo Lengai. *J Petrol* 36:869–889
- Dawson JB, Pinkerton H, Norton GE, Pyle D (1990) Physicochemical properties of alkali carbonatite lavas: data from the 1988 eruption of Oldoinyo Lengai, Tanzania. *Geology* 18:260–263
- Dawson JB, Pinkerton H, Pyle DM, Nyamweru C (1994) June 1993 eruption of Oldoinyo Lengai, Tanzania; exceptionally viscous and large carbonatite lava flows and evidence for coexisting silicate and carbonate magmas. *Geology* 22:799–802
- Duncan AM, Guest JE, Stofan ER, Anderson SW, Pinkerton H, Calvari S (2004) Development of tumuli in the medial portion of the 1983 aa flow-field, Mount Etna, Sicily. *J Volcanol Geotherm Res* 132:173–187
- Duraiswami RA, Bondre NR, Dole G, Phadnis VM, Kale VS (2001) Tumuli and associated features from western Deccan Volcanic Province, India. *Bull Volcanol* 63:435–442
- Ferri F, Burlini L, Cesare B, Sassi R (2007) Seismic properties of lower crustal xenoliths from El Hoyazo (SE Spain): experimental evidence up to partial melting. *Earth Plan Sci Lett* 253:239–253
- Fornari DJ, Malahoff A, Heezen BC (1978) Volcanic structure of the crest of the Puna Ridge, Hawaii: geophysical implications of submarine volcanic chain. *Geol Soc Am Bull* 89:605–616
- Guilbaud M-N, Blake S, Self S, Thordarson T, Keszthelyi L (2006) Internal textures and cooling histories of rubbly pahoehoe lavas. A George P.L. Walker symposium on *Advances in Volcanology, IAVCEI, Reykholt, Iceland, Abstract volume* p. 14
- Gudmundsson A (2004) Effects of Young's modulus on fault displacement. *Comptes Rendus—Geoscience* 336:85–92
- Gudmundsson A, Philipp SL (2006) How local stress fields prevent volcanic eruptions. *J Volcanol Geotherm Res* 158:257–268
- Hon K, Kauahikaua J, Denlinger R, MacKay K (1994) Emplacement and inflation of pahoehoe sheet flows: Observations and measurements of active lava flows on Kilauea Volcano, Hawaii. *Geol Soc Am Bull* 106:351–370
- Huppert HE, Sparks RSJ (1985) Komatiites I: emplacement and flow. *J Petrol* 26:694–725

- Jarvis RA (1995) On the cross-sectional geometry of thermal erosion channels formed by turbulent lava flows. *J Geophys Res* 100:10127–10140
- Keller J, Krafft M (1990) Effusive natrocarbonatite activity of Oldoinyo Lengai, June 1988. *Bull Volcanol* 52:629–645
- Kervyn M, Ernst GGJ, Klaudius J, Keller J, Kervyn F, Mattsson HB, Belton F, Mbede E, Jacobs P (2008) Voluminous lava flows at Oldoinyo Lengai in 2006: Chronology of events and insights into the shallow magmatic system. *Bull Volcanol* DOI 10.1007/s00445-007-0190-x
- Klaudius J, Keller J (2006) Peralkaline silicate lavas at Oldoinyo Lengai, Tanzania. *Lithos* 91:173–190
- Mattsson HB, Höskuldsson Á (2005) Eruption reconstruction, formation of flow-lobe tumuli and eruption duration in the 5900 BP Helgafell lava field (Heimaey), south Iceland. *J Volcanol Geotherm Res* 147:157–172
- Norton G, Pinkerton H (1997) Rheological properties of natrocarbonatite lavas from Oldoinyo Lengai, Tanzania. *European J Min* 9:351–364
- Oddsson B (1984) Geology and geotechnical behaviour of the young volcanic rocks of Iceland with emphasis on the effects of petrography. PhD Thesis. ETH, Zürich (in German)
- Pinkerton H, Norton GE, Dawson JB, Pyle DM (1995) Field observations and measurements of the physical properties of Oldoinyo Lengai alkali carbonatite lavas, November 1988. In: Bell K, Keller J (eds) *Carbonatite volcanism of Oldoinyo Lengai—Petrogenesis of natrocarbonatite*. Springer, Berlin, pp 23–36
- Rossi M, Gudmundsson A (1996) The morphology and formation of flow-lobe tumuli on Icelandic shield volcanoes. *J Volcanol Geotherm Res* 72:291–308
- Rowland SK, Walker GPL (1987) Toothpaste lava: Characteristics and origin of a lava structural type transitional between pahoehoe and aa. *Bull Volcanol* 49:631–641
- Self S, Keszthelyi L, Thordarson T (1998) The importance of pahoehoe. *Ann Rev Earth Plan Sci* 26:81–110
- Thordarson Th, Self S (1998) The Roza member, Columbia River basalt group: a gigantic pahoehoe lava flow field formed by endogenous processes? *J Geophys Res* 103:27411–27445
- Umino S, Lipman PW, Obata S (2000) Subaqueous lava flow lobes, observed on ROV KAIKO dives off Hawaii. *Geology* 28:503–506
- Walker GPL (1991) Structure, and origin by injection of lava under surface crust, of tumuli, “lava rises”, “lava-rise pits”, and “lava-inflation clefts” in Hawaii. *Bull Volcanol* 53:546–558
- Wilmoth RA, Walker GPL (1993) P-type and S-type pahoehoe: a study of vesicle distribution patterns in Hawaiian lava flows. *J Volcanol Geotherm Res* 55:129–142
- Zaitsev AN, Keller J (2006) Mineralogical and chemical transformation of Oldoinyo Lengai natrocarbonatites, Tanzania. *Lithos* 91:191–207